

Influence of Nanomaterial Fillers in Biopolymer Electrolyte System for Squaraine-based Dye-Sensitized Solar Cells

Stephanie Chan, Jose Paolo Bantang, Drexel Camacho*

Chemistry Department, De La Salle University, 2401 Taft Avenue, Manila, Philippines

*E-mail: drexel.camacho@dlsu.edu.ph

Received: 20 May 2015 / Accepted: 29 June 2015 / Published: 28 July 2015

The vast use of fossil fuel demands the development of new sources of renewable energy. Dye-sensitized solar cells (DSSCs) have been extensively studied due to their competitive cost, ease of fabrication, high degree of tunability and relatively good-energy conversion efficiencies. The performance and stability of DSSCs are limited by leakage and solvent evaporation. This study explores the effects of nanofillers in the performance of dye-sensitized solar cells by incorporating nano-sized titanium dioxide, iron (III) oxide and halloysite fillers into the polymer electrolytes based on κ -carrageenan/DMSO/TBAI:I₂. Optimization and characterization of various concentrations of fillers were done before incorporation in solar cells. The effect of ionic conductivity and diffusion coefficient to the overall conversion efficiency of the cells were studied. The effect of squaraine dye was also investigated. The addition of various fillers to the polymer electrolyte system increased the dissociation of iodide ions and improved the ionic conductivity of the cells. The diffusion coefficient of tri-iodide ions was also greatly enhanced because of the increased volume of the system brought about by reducing polymer-polymer interaction, which increased the mobility of the redox couple (I₃⁻/I⁻). DSSC characterization revealed a low efficiency due to a relatively high charge transfer resistances at the TiO₂/dye/electrolyte interface.

Keywords: dye-sensitized solar cells, κ -carrageenan, biopolymer electrolyte

1. INTRODUCTION

Solar power is one of the most promising solutions to the increasing demands for energy. Conventional silicon-based solar cells convert sun's energy to electricity with efficiency as high as 24% using very expensive Si of high purity [1]. Despite its energy conversion capacity, mass utilization of silicon-based solar cells is a major challenge due to prohibitive production cost. Alternatively, dye-sensitized solar cells are potentially less expensive, easy to fabricate and shows

relatively good efficiencies at high temperatures [2]. DSSC configuration consists of a thin film of metal oxide semiconductor deposited on a fluorine-doped tin oxide (FTO) glass and treated with dye sensitizer that acts as a photo anode. The liquid electrolyte containing iodide/tri-iodide (I/I_3^-) redox couple is sandwiched between the photo anode and the counter-electrode, which is a platinum-coated FTO glass. Through excitation of dye electrons from the valence band into the conduction band, it is able to convert energy from sunlight. The dye captures visible light and as the dye molecule is excited, the electrons are injected into the semiconductor to the external load. The photo-excited dye is re-established to its ground state by receiving an electron from the electrolyte system, which undergoes a redox process. The donated electron of the iodide (I^-) is subsequently restored by the reduction of tri-iodide (I_3^-) at the counter-electrode. The platinum coating from the counter electrode acts as a catalyst for the reduction of tri-iodide [3].

Current studies show that the inclusion of inorganic nanomaterial filler in polymer electrolyte improves the ionic conductivity, transport properties and mechanical properties [4]. The enhancement of these properties depends on the particle size, shape and crystallinity of the nanofiller materials. Researchers proved that the filler provides a solid like support matrix that allows the amorphous polymer to uphold its liquid-like characteristics resulting to a faster ionic mobility [5]. As a result, it could help enhance the overall performance of the cells and further increase the stability. This study investigates the influence of various fillers specifically nano-sized titanium dioxide, iron (III) oxide and halloysite on the overall performance of the cell using biopolymer electrolyte in organic dye-sensitized solar cells.

2. METHODOLOGY

2.1. Preparation of the Biopolymer Electrolytes

In the preparation of the biopolymer electrolyte, 0.010g of κ -carrageenan (Mioka Bioassay) was dissolved in 1mL of dimethyl sulfoxide (Aldrich). The solution was heated in a microwave for one minute and then at 80.0°C using a hot plate for a few minutes to ensure the dissolution of carrageenan in the solvent. Afterwards, 0.369g of tetrabutylammonium iodide (TBAI) and 0.064g I_2 from Aldrich were added to the solution. The solution was then heated again in a hot plate at 80.0°C. This solution acted as the control.

2.2. Preparation of the Biopolymer Electrolytes with Fillers

The inorganic nanofillers namely titanium dioxide (10-25nm, US Nano), iron (III) oxide (<50nm, Aldrich) and natural halloysite (ITDI-MSD) were added to the prepared liquid electrolyte system described above. Specific concentrations of titanium dioxide used were 0.2%, 0.4%, 0.6%, 0.8%, 1.0%, 1.2%, 1.4%, 1.6%, 1.8% and 2.0%w/v. As for the iron (III) oxide and halloysite clay, the concentrations used were 0.2%, 0.4%, 0.6%, 0.8% and 1.0%w/v. After the addition of the filler, the solution was heated at 80.0°C.

2.3. Preparation of the Dye Sensitizers

The dye solution was prepared by dissolving squaraine (Solaronix) in 25 mL ethanol forming a final concentration of 0.6 M. The dye solutions were kept in an airtight container at room temperature and away from sunlight.

2.4. Cell Assembly

In the fabrication of the dye-sensitized solar cell, the FTO glasses were cut into 2 cm x 2 cm size. The glass plates were washed with ethanol for 15 mins using a sonicator followed by air drying and oven drying. The resistance of the glass plates ($\sim 10\Omega$) was measured using a multi-meter set to check the conductive side. With the conductive side facing up, strips of Scotch Magic tape #810 were attached to the edges of the glass plate. Using the doctor blade technique, the TiO_2 paste was deposited in the middle of the glass. The adhesive tapes were removed before placing the glass plates in a muffle furnace for 30mins at 450°C . After sintering, the glass plates were cooled at 60°C and subsequently immersed in the dye solution (0.6 M squaraine dye (SQ2)) to adsorb the dye on TiO_2 layer. For the counter electrode (FTO glass, 2 cm x 2 cm), an alcoholic solution of platinum (Platisol, Solaronix) was applied on the FTO conductive side using brush. It was sintered on a muffle furnace for 30 mins at 450°C followed by slow cooling. In preparation of the open cell configuration, two drops of the biopolymer electrolyte system was sandwiched in between the photo anode and the counter-electrode with the coated sides facing each other. Paper binders were used to hold the electrodes together.

2.5. Measurements

2.5.1. Linear Sweep Voltammetry

Linear sweep voltammetry measurements with various concentrations of fillers were performed to study the diffusion coefficient of the tri-iodide ions in the electrolyte system. The measurement was done using a cell consisting of the biopolymer electrolyte sandwiched between two FTO platinized glass plates (active area: $1 \times 1 \text{cm}^2$). The limiting current was obtained from the linear sweep voltammetry curves using a Metrohm Autolab potentiostat (PGSTAT128N). The measurements were performed in the -1.0 to 1.0 V voltage range, with a scan rate of 10mV/s. Triplicate measurements were performed. The tri-iodide diffusion coefficient $D_{\text{I}_3^-}$, was calculated using the equation:

$$J_{\text{lim}} = \frac{2nFC_0D_{\text{I}_3^-}^*}{d}$$

Where $n = 2$ (the number of electrons involved in the electrochemical redox reaction of tri-iodide to iodide); F is the Faraday's constant, d the distance between the two electrodes and C_0 the initial molar concentration of tri-iodide ions [6].

2.5.2. Ionic Conductivity

Using similar FTO-Pt/biopolymer/Pt-FTO cell, with spacer of 50 μ m, the ionic conductivity of biopolymer electrolyte with different nanofiller concentrations were characterized using electrochemical impedance spectroscopy (EIS) (Metrohm Autolab potentiostat PGSTAT128N) equipped with a frequency response analyzer module (FRA23M Module). Impedance tests were performed at room temperature in a frequency range between 0.1Hz to 1,000,000 Hz at 10 frequencies per decade with amplitude of 0.01V. Triplicate measurements were performed. The conductivity was obtained using the equation:

$$\sigma = \frac{L}{AR_b}$$

The resistance (R_b) is determined as the intercept of the Nyquist plot against the real part of the impedance. The active area "A" is 1x1cm² and L is the 50 μ m thickness of the spacer [7]. The impedance response was analyzed using the fitting program provided by the Autolab.

2.5.3. Efficiency

The efficiency of the fabricated DSSCs was analyzed under AM1.5 solar simulator (Abet Technologies; 100mW/cm²). An Autolab potentiostat was used to record the current-voltage (I-V) characteristics [8]. The start potential was set to -0.800V, stop potential at 0.00V, and scan rate at 10mV. The open circuit voltage (V_{oc}), short circuit current (I_{sc}) and fill factor (FF) were obtained from the I-V curve and the efficiency of the cell (η) was calculated.

2.5.4. AC impedance

The impedance parameters of the biopolymer electrolyte with various nanofillers in the presence of the dye were measured using linear sweep voltammetry with the following conditions: start potential at -0.800V, stop potential at 0.00V and scan rate of 10mV using a 2.75mW/cm² (35kW) halogen lamp light source.

3. RESULTS AND DISCUSSION

3.1. Ionic Conductivity and Diffusion Coefficient Measurements of Biopolymer Electrolyte Systems

The Nyquist plot was interpreted into an equivalent circuit model (Figure 1) representing the solution resistance, charge transfer resistance, Warburg impedance and constant phase element [9]. This circuit model was applied to all measurements and the ionic conductivity of the nanofilled electrolyte systems was measured.

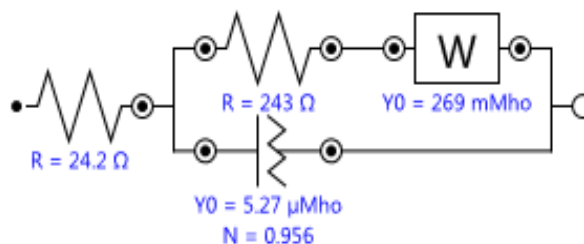


Figure 1. Equivalent circuit model for the liquid polymer electrolytes

The solution resistances (Table 1) measured for various concentrations of the nanofillers relative to the control (24.2Ω), revealed that the addition of 1.4% TiO₂, 0.4% Fe₂O₃ and 0.2% halloysite gave the lowest resistances of 14.8Ω, 18.8Ω and 14.7Ω, respectively.

Table 1. Solution resistances (Ω) of biopolymer electrolyte with nanofillers

Concentration	TiO ₂	Fe ₂ O ₃	Halloysite
0.0% (control)	24.158	24.158	24.158
0.2%	-	27.508	14.659
0.4%	45.825	18.822	17.029
0.6%	26.006	22.585	19.997
0.8%	21.276	20.020	19.402
1.0%	20.023	19.660	18.292
1.2%	17.381	-	-
1.4%	14.844	-	-
1.6%	25.912	-	-

These values are supported by the low Warburg impedance relative to the control indicating that the electrolyte systems with fillers have efficient movement of electrons. This suggests that fast reduction of tri-iodide to iodide ions by two electrons occur at the platinum electrode (Figure 2).

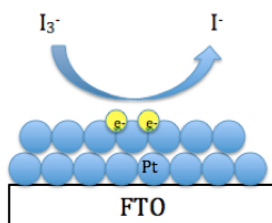


Figure 2. Mechanism of the reduction of tri-iodide to iodide ions

The ionic conductivity using the optimized concentration of nanofilled electrolyte system (Figure 3) has shown improved conductivity compared to that of the control (2.61x10⁻⁴ S/cm).

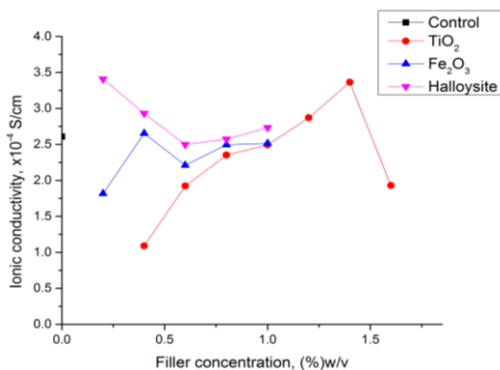


Figure 3. Ionic conductivity of biopolymer electrolyte with various concentrations of fillers

This improvement can be attributed to the proposed interaction between the biopolymer electrolyte and filler (Figure 4) forming an interface in between that helps the dissociation of iodide ion from TBA⁺ [10]. This separation not only enhances the ionic conductivity of the electrolyte but importantly, increases the interaction of 2I⁻ and I₂ promoting the Grotthuss mechanism for the formation of redox couple I⁻ and I₃⁻. Nevertheless, high concentrations of fillers reduce this effect as repulsion between sulfate groups and the excess tri-iodide/iodide ions have a much greater effect.

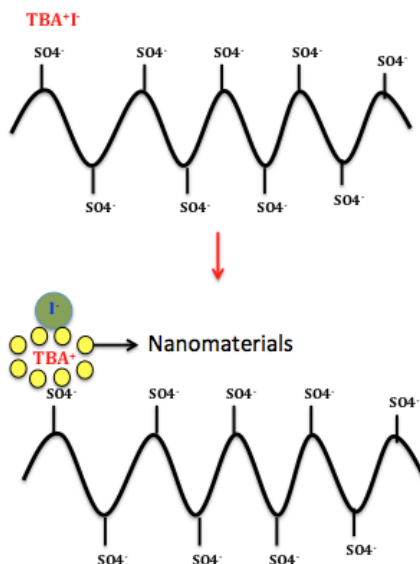


Figure 4. Proposed Mechanism of the separation of iodide ions

The diffusion coefficients of the I⁻/I₃⁻ redox couple in the biopolymer electrolyte system with and without fillers were determined using linear sweep voltammetry by measuring the limiting current densities (Figure 5). Due to a large excess of iodide ions in the electrolyte, only the diffusion of tri-iodide ions limits the current. Thus, the limiting current density is obtained merely at the oxidation process. The control was found to have a diffusion coefficient of 3.13x10⁻⁷ cm²/S. The addition of

fillers improved the diffusion coefficient to $3.47 \times 10^{-7} \text{ cm}^2/\text{S}$, $3.63 \times 10^{-7} \text{ cm}^2/\text{S}$, $3.26 \times 10^{-7} \text{ cm}^2/\text{S}$ with 1.4% TiO_2 , 0.4% Fe_2O_3 and 0.2% halloysite, respectively.

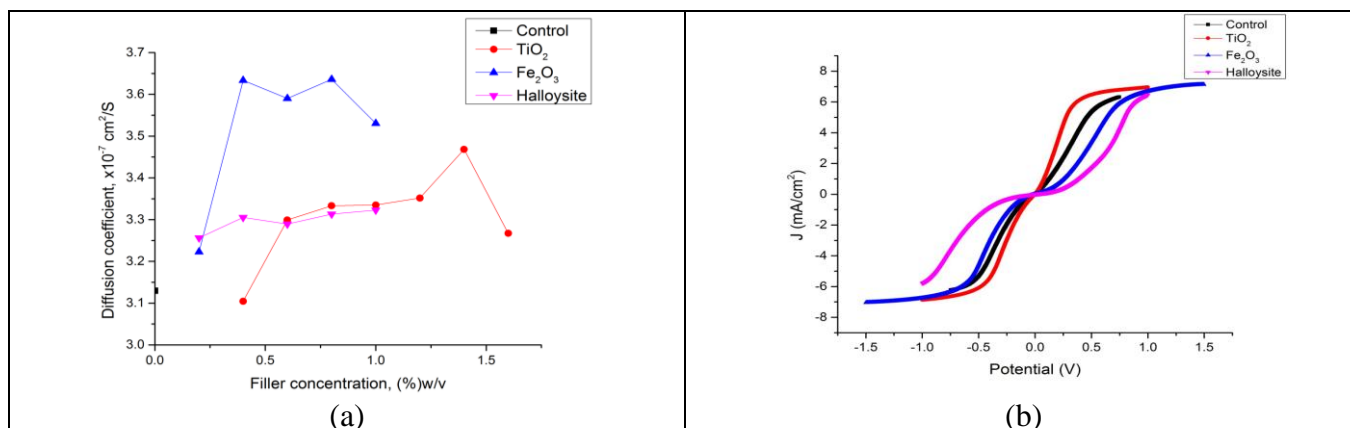


Figure 5. (a) Diffusion coefficient of biopolymer electrolyte with various concentrations of fillers; and (b) LSV of the optimized biopolymer electrolyte with fillers

The enhanced diffusion coefficient indicates a fast mobility of ions carrying the electrons in the electrolyte system. The inclusion of fillers increased the volume of the system as it remains in between the polymer chains. Furthermore, it reduces polymer-polymer chain interaction in the system [11]. Size limitation is also a factor in the transport properties. Among the three fillers, the halloysite gave the lowest diffusion coefficient that can be attributed to the particle size of halloysite, which is larger than titanium dioxide and iron (III) oxide.

3.2. Photovoltaic Performance of the Carrageenan Based DSSCs with Optimized Concentration of Fillers

The nanomaterials in carrageenan-based polymer electrolyte systems were incorporated in DSSC using squaraine dye as sensitizer. Squaraine dye absorbs between 253nm to 652nm with λ_{max} at 652nm. The nanomaterials have no notable absorptions except for iron (III) oxide, which has an absorption wavelength at the range of 206-340nm with λ_{max} at 258nm.

Solar cells containing the prepared biopolymer electrolyte with and without fillers were fabricated. The optimized concentrations of the fillers were chosen based on the computed ionic conductivity and diffusion coefficient. The solar cell parameters based on I-V curves of the DSSCs (Table 2), showed that the control has a higher efficiency compared to the electrolytes with fillers. The low efficiency can be attributed to the low open circuit voltage and short circuit current. The drop in short circuit current could be due to the inefficient charge transfer in the platinum/electrolyte interface. Additionally, the decrease in efficiency with the addition of iron (III) oxide can be ascribed to its overlap in absorption with the dye sensitizers competing for the electrons to reduce itself to iron (II). With halloysite, the efficiency also decreased due to the drop in the short circuit current, which

exhibits a lower ability to enhance chemical reactions damaging the reduction process of the redox couple (I_3^-/I^-). Furthermore, the decrease in efficiency may also be caused by solubility limitation of the halloysite molecules in the electrolyte solution. Likewise, the low efficiency observed using squaraine dye is due to the weak absorption capability of organic dyes [12].

Table 2. I-V Characteristics of solar cells for liquid polymer electrolyte with and without fillers in organic dye-sensitizer

Filler	V_{oc} (V)	I_{sc} (mA/cm ²)	FF	η (%)
Control	0.751	1.91	0.571	0.819
TiO ₂	0.751	1.83	0.557	0.765
Fe ₂ O ₃	0.687	3.96	0.074	0.202
Halloysi te	0.741	1.39	0.503	0.518

3.3. Electrochemical Characterization of the Carrageenan Based DSSCs with Optimized Concentration of Fillers

The dye-sensitized solar cell using electrolyte systems with the incorporation of various fillers in squaraine dyes was characterized by ac impedance spectroscopy (Figures 6). The Nyquist plots obtained showed only one semi-circle plots. By fitting the impedance data to an equivalent circuit model (Figure 7), the electronic processes of the cell were described [13].

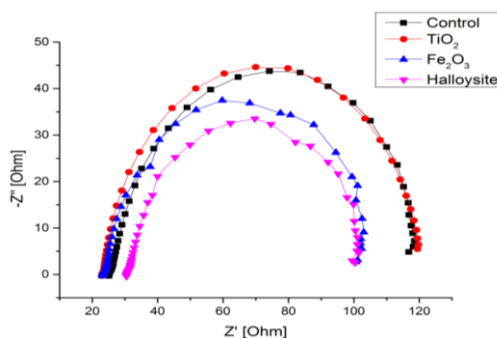


Figure 6. AC impedance analysis of the biopolymer electrolytes with and without fillers in squaraine dye under halogen lamp illumination

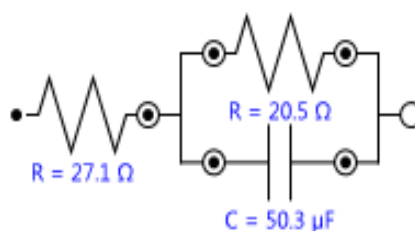


Figure 7. Equivalent circuit model for the liquid polymer electrolytes

Table 3. AC impedance parameters of solar cells for biopolymer electrolyte with and without fillers in organic dye-sensitizer

Filler	Squaraine (SQ2)	
	Solution resistance (R_s), Ω	Charge transfer resistance at TiO_2 /dye/electrolyte interface (R_{TiO_2}), Ω
Control	26.179	90.787
TiO ₂	23.705	93.598
Fe ₂ O ₃	24.130	77.692
Halloysite	31.510	68.912

The ac impedance parameters (Table 3) showed that the addition of titanium dioxide decreases the solution resistance showing a more efficient mobility of the total ions in the cell. Moreover, it has an increased charge transfer resistance indicating more electron recombination at the TiO_2 /dye/electrolyte interface relative to the control [14, 15]. Despite the decreased solution resistance, the overall efficiency is lower compared to the control. This could also be due to the electron transport properties at other interfaces, which were not studied in this research. Among the three nanofillers however, the addition of TiO_2 showed the highest efficiency consistent with low solution resistances. With the addition of iron (III) oxide, the charge transfer resistance has improved in SQ2 dye, which shows that there is not much electron recombination happening at the TiO_2 with SQ2/electrolyte interface. The overall efficiency of the cell however is still lower compared to the control. Moreover, the unfavorable results for Fe_2O_3 can also be attributed to compounding interplay of factors such as absorption overlap and the potential aggregation of ions since iron (III) oxide is known to have a low isoelectric point of 6.5-6.8. Hence, iron (III) oxide in electrolyte (pH 6-8) would obtain a negative charge on its surface, which attracts strongly the cations [16] forming an aggregate (Figure 8).

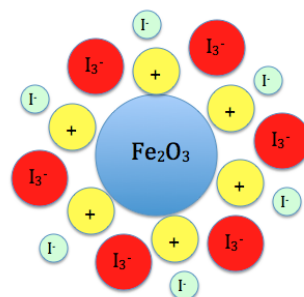


Figure 8. Probable structure of iron (III) oxide suspended in liquid polymer electrolyte

The halloysite addition to the biopolymer electrolyte in squaraine dye was found to have higher solution resistance and lower charge transfer resistance than the control affecting the electron recombination reaction that occurs between TiO_2 /dye/electrolyte interfaces [17]. It is also possible that

the excess tri-iodide/iodide ions have greater repulsive forces with the sulfate groups of κ -carrageenan and hydroxyl groups in halloysite than the attraction between the hydroxyl group and TBA^+ . The overall efficiency of the cell is still low due to the unfavorable movement of the electrons at other interfaces of the cell.

4. CONCLUSIONS

In this study, a biopolymer electrolyte based on κ -carrageenan containing tri-iodide/iodide redox couple was modified for dye-sensitized solar cell applications. Electrolyte systems incorporated with inorganic nanofillers such as titanium dioxide, iron (III) oxide and halloysite were optimized and characterized. The inclusion of fillers resulted in an increased ionic conductivity of the electrolyte system indicating a fast mobility of ions in the polymer electrolyte system. Furthermore, the diffusion coefficient increased exhibiting the fast mobility of the iodide/tri-iodide redox couple as the fillers assist in the dissociation of the iodide ions from the counter cations. The inclusion of the three fillers to the κ -carrageenan/DMSO/TBAI:I₂ as polymer electrolyte system in dye-sensitized solar cells resulted in low efficiency relative to using a polymer electrolyte without fillers. The low efficiency measured with the inclusion of titanium dioxide nanofiller can be attributed to the low short-circuit current due to enhanced recombination reaction.

ACKNOWLEDGEMENTS

The authors are grateful to Dr. Erwin Enriquez, Dr. Arnel Salvador, Dr. Armando Somintac for the use of solar simulator and Ms. Anna San Esteban for guidance in solar measurements. The technical assistance in the instrumental laboratory by Michael Ajero and Rey Correa are acknowledged. Halloysite was kindly provided by Dr. Blessie Basilla of DOST-ITDI MSD. This work was supported by research grants from DOST-PCIEERD, DLSU Science Foundation and DLSU-URCO.

References

1. S. Gunes and N. S. Sariciftci, *Inorganica Chimica Acta*, 361 (2008) 581-588.
2. A.H.T. Le, S. Ahn, S. Han, J. Kim, S.Q. Hussain, H. Park, C. Park, C.P.T. Nguyen, V.I. Dao and J. Yi, *Solar Energy Materials and Solar Cells*, 125 (2014) 176-183.
3. D. Wei, *International Journal of Molecular Sciences*, 11 (2010) 1103-1113.
4. M. Gratzel, *Journal of Photochemistry and Photobiology C: Photochemistry Reviews*, 4 (2003), 145-153.
5. M.S. Akhtar, J.M. Chun and O.B. Yang, *Electrochemistry Communication*, 9 (2007) 2833-2837.
6. M.S. Kang, K.S. Ahn and J.W. Lee, *Journal of Power Sources*, 180 (2008) 896-901.
7. S.Y. Cha, Y.G. Lee, M.S. Kang and Y.S. Kang, *Journal of Photochemistry and Photobiology A: Chemistry*, 211 (2010) 193-196.
8. Q. Wang, J.E. Moser and M. Gratzel, *J. Phys. Chem. B*, 109 (2005) 14945-14953.
9. F. Bella, E.D. Ozzello, A. Sacco, S. Bianco and R. Bongiovanni, *International Journal of Hydrogen Energy*, 39 (2014) 3036-3045.
10. S.K. Deraman, N.S. Mohamed and R.H.Y Subban, *International Journal of Electrochemical Science*, 8 (2013) 1459-1468.

11. E. Charzivasiloglou, T. Stergiopoulos, A.G. Kontos, N. Alexis, M. Prodromidis and P. Falaras, *Journal of Photochemistry and Photobiology A: Chemistry*, 192 (2007) 49-55.
12. S. Hwang, J.H. Lee, C. Park, H. Lee, C. Kim, C. Park, M.H. Lee, W. Lee, J. Park, K. Kim, N.G. Park and C. Kim, *ChemComm*, (2007) 4887-4889.
13. J.S. Im, S.K. Lee and Y.S. Lee, *Applied Surface Science*, 257 (2011) 2164-2169.
14. W. Qin, S. Lu, X. Wu and S. Wang, *International Journal of Electrochemical Science*, 8 (2013) 7984.
15. R. Kern, R. Sastrawan, J. Ferber, R. Stangl, R. *Electrochimica Acta* 47, (2002). 4213–4225.
16. S.M. Mohanty and P. Bhargava, *Electrochimica Acta*, 90 (2013) 291-294.
17. S. Nakade, T. Kanzaki, W. Kubo, T. Kitamura, Y. Wada and S. Yanagida, *Journal of Physical Chemistry B*, 109 (2005) 3480-3487.

© 2015 The Authors. Published by ESG (www.electrochemsci.org). This article is an open access article distributed under the terms and conditions of the Creative Commons Attribution license (<http://creativecommons.org/licenses/by/4.0/>).